ELSEVIER

Neurocomputing 38–40 (2001) 343–350

NEUROCOMPUTING

www.elsevier.com/locate/neucom

Dendritic morphology and signal delay in superior colliculus neurons

Andreas Schierwagen*, Conny Claus

Institut für Informatik, Universität Leipzig, PO Box 100920, 04009 Leipzig, Germany

Abstract

Experimental data derived from two classes of superior colliculus neurons—deep layer neurons (DLNs) and superficial layer neurons (SLNs)—have been used to study the influence of dendritic anatomy on synaptic input processing. Anatomical measures of dendrites were first determined. Compartmental neuron models (3 of each class) were built to estimate passive membrane parameters and to calculate functional characteristics of synaptic input (attenuation, delay and time window). The two cell classes show distinct differences both in morphological and functional characteristics. While the functional parameters derived on SLNs are compatible with time-critical functions, DLNs in contrast show integrator traits.. © 2001 Elsevier Science B.V. All rights reserved.

Keywords: Superior colliculus; Dendritic anatomy; Postsynaptic signals; Delays

1. Introduction

The superior colliculus (SC) is a part of the mammalian midbrain involved in sensory-motor control. In dependence on neuron localization within the SC, their dendrites show distinct branching patterns in the deep and superficial layers, respectively (Fig. 1). These structural differences are correlated with distinct functions in information processing: deep layer neurons (DLNs) obtain multimodal afferences whereas superficial layer neurons (SLNs) receive exclusively visual input.

Basic to the present study are correlated morphological and electrophysiological data on different classes of SC neurons previously published [2,3,6,7]. These neurons have been used as a model system to study the interplay of dendritic anatomy and

* Corresponding author.

PII: S0925-2312(01)00417-9

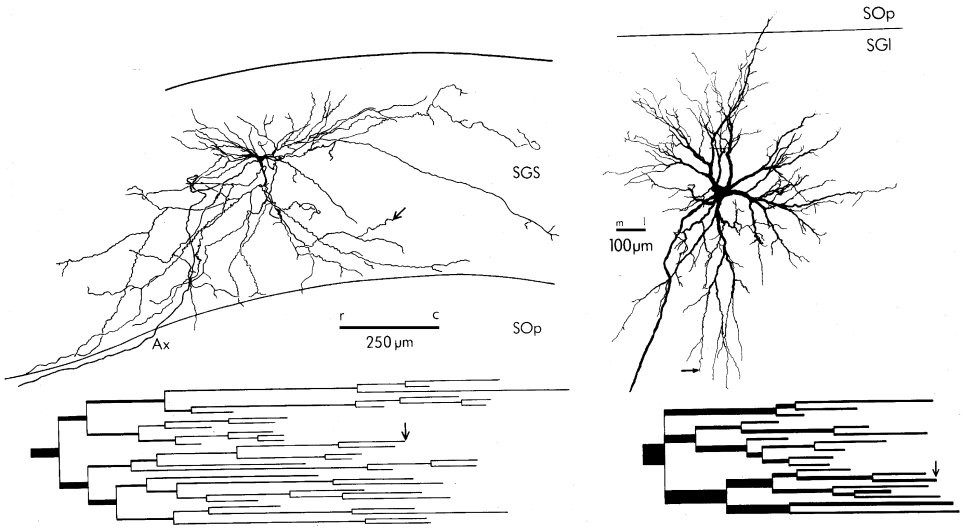

Fig. 1. Dendritic ramification pattern of superior colliculus neurons. Displayed are camera lucida drawings of one superficial (*cell* $\frac{4}{6}$, *left*) and one deep layer neuron (*cell pb1*, *right*) each, together with Sholl diagrams of one dendrite (arrows).

signal processing. Dendritic trees are known as a source of time delays and attenuation in single neurons. In a first step, we investigated their morphological features. Then we built compartmental models of each SC cell. These models were used in two ways: to solve the "inverse problem" and to do "forward computations" [5]. To determine (passive) membrane parameters, data from current injection experiments are compared with the simulation responses of the compartmental models (inverse problem). In the forward computations, the estimated parameters are employed to compute functional characteristics such as attenuation, delay and time window of synaptic input signals. In this way, we tried to get clues for the potential function of SLNs and DLNs as integrators or coincidence detectors.

2. Theoretical basis

Agmon-Snir [1] introduced a new approach for analyzing dendritic transients, in particular time delays and attenuation. In this method, the various moments of a transient signal are used to characterize the signal properties. The following definitions are all based on the moments of signals:

kth moment of a signal $f(t)$: $\quad m_{f,k} := \int_{-\infty}^{\infty} t^k \cdot f(t)\,\mathrm{d}t,$

Strength of a signal $f(t)$: $\quad \widehat{s}_f := \int_{-\infty}^{\infty} f(t)\,\mathrm{d}t = m_{f,0},$

Centroid of a signal $f(t)$: $\widehat{t}_f := \int_{-\infty}^{\infty} t \cdot f(t)\,\mathrm{d}t / \int_{-\infty}^{\infty} f(t)\,\mathrm{d}t = m_{f,1}/m_{f,0}$,

Dispersion of a signal $f(t)$: $\widehat{\sigma}_f^2 := \int_{-\infty}^{\infty} (t - \widehat{t})^2 \cdot f(t)\,\mathrm{d}t / \widehat{s}_f = m_{f,2}/\widehat{s}_f - \widehat{t}_f^2$,

Time window of a signal $f(t)$: $\widehat{w}_f := [\widehat{t}_f - \widehat{\sigma}_f, + \widehat{t}_f + \widehat{\sigma}_f]$.

Let x be the site of current input and y the recording site. Using the above definitions, relations for signal attenuation and time delay can be derived, as illustrated in Fig. 2.

3. Methods

All data were obtained from neurons recorded intracellularly and stained with HRP as described in [2,3]. The sample of cells selected for analysis comprised three SLNS and three DLNs. In addition, data from another sample of electrophysiologically examined SC cells were used.

The morphological features of SC neurons were investigated as differentiated into metrical and topological ones. The simulation package NEURON was used to built compartmental models of the six SC cells. To determine the passive membrane parameters, data from current injection experiments were compared with the simulation responses of the compartmental models. Systematic parameter variations

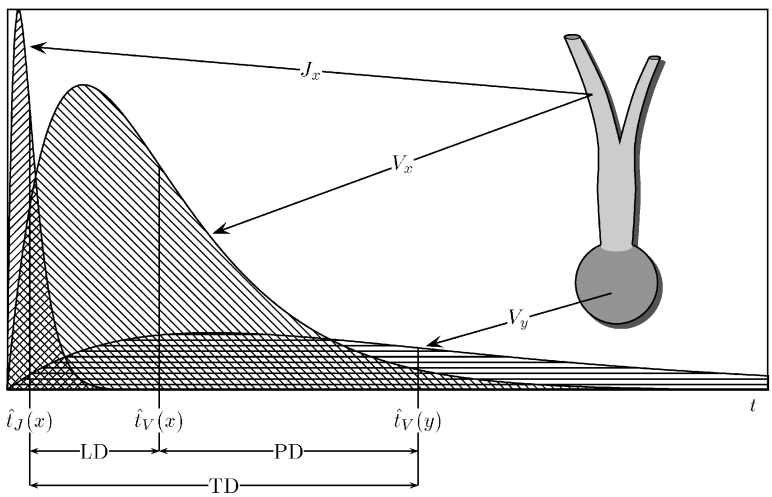

Fig. 2. Illustration of delay types. A current J_x of α-function shape is injected at point x, and the voltage reponses V_x and V_y at x and at another location y are shown. Strengths of signals are indicated by hatched area; vertical lines correspond to centroids. Delays are defined as follows: local delay $LD(x) := \widehat{t}_V(x) - \widehat{t}_I(x)$, propagation delay $PD(x,y) := \widehat{t}_V(y) - \widehat{t}_V(x)$, transfer delay $TD(x,y) := \widehat{t}_V(y) - \widehat{t}_I(x)$.

revealed several regions of parameter space in which the SC neuron models fit the data. We resolved this non-uniqueness by applying constraints from independent studies on realistic values of membrane capacitance, internal resistivity and somatic shunt. Using our matrix-moment method [4], we computed the functional characteristics signal attenuation, delay and time window.

4. Results

4.1. Morphology

The two cell classes show distinct differences in their morphology, as exemplified by Fig. 1. In the mean, total surface area A_N and volume of DLNs exceed that of SLNs by a factor of 4 and 2.8, respectively. The ratio of dendritic to somatic surface area A_D/A_S in SLNs is almost twice that of DLNs. For similar electrical properties this would mean that in DLNs the soma represents a stronger electrical load as compared with SLNs. Mean dendritic path lengths l_{mean} of SLNs are larger, and dendritic branch diameters d_{mean} are smaller than those of DLNs (Table 1).

With respect to topology (branching pattern) we have the following findings: (i) the number of stem dendrites is 3–6 and 7–10, (ii) the maximal branching order is 10–12 and 6–9 in SLNs and DLNs, respectively, (iii) the mean number of terminal segments is about 110 in both SLNs and DLNs. For all cells of the two classes the mean of branching exponents is near 1.5 (for details, see [8]).

4.2. Parameter search

For each of the 6 cells the input resistance R_N is known from experiments. Time constants were estimated from another sample of collicular neurons. The average of time constants τ_m is 4.1 ms (range 2.4–8.0 ms) and 4.5 ms (range 3.0–5.8 ms) in SLNs and DLNs, respectively. From these known parameters we computed the 3 or 4 unknown parameters membrane capacity C_m, membrane resistance R_m (uniform or nonuniform) and axial resistivity R_i. We found several admissible combinations of

Table 1
Results of parameter search for SLNs ($\frac{7}{4}$, $\frac{4}{1}$, $\frac{4}{6}$) and DLNs (af, pb1, pb2)[a]

Cell no.	A_N ($\times 10^3$ μm^2)	A_D/A_S	l_{mean} (μm)	d_{mean} (μm)
4/1	40.1	20.9	660	0.8
4/6	83.8	23.9	936	1.2
7/4	22.4	15.5	484	0.5
af	151.7	7.8	351	3.7
pb1	186.3	17.6	440	2.6
pb2	79.5	10.7	313	2.3

[a] $A_N \sim$ total neuron surface area, $A_D/A_S \sim$ dendrite-to-soma surface area ratio, $l_{mean} \sim$ mean dendritic path length, $d_{mean} \sim$ mean dendritic branch diameter.

parameters which fitted the experimental data equally well. From these sets we selected regions of parameter combinations which could be considered reasonable: $1\ \mu F/cm^2 \leqslant C_m \leqslant 2\ \mu F/cm^2$, $100\ \Omega\,cm \leqslant R_i \leqslant 500\ \Omega\,cm$. This yielded at least three admissible combinations for each SLN and DLN (Table 2).

4.3. Forward calculations

In order to estimate the impact which a specific set of model parameters might have on the functional characteristics derived, forward calculations were performed with each set of admissible parameter combinations. A particular parameter combination is uniquely identified by the corresponding resistivity value R_i. Thus, in Tables 3 and 4 simulations are distinguished by cell number, followed by the corresponding resistivity value R_i. We used as input an α-shaped current (duration: 2 ms, $g_{max} = 0.1$ S).

Attenuation. The attenuation values of all dendritic input locations are not normally distributed, and for both somatopetal and somatofugal attenuations the distribution functions are different for the 2 cell groups. Attenuation in SLNs is generally larger if compared with DLNs. Somatopetal signals from dendritic tips are heavily diminished at the soma.

Table 2
Results of parameter search for SLNs ($\frac{4}{1}$, $\frac{4}{6}$, $\frac{7}{4}$) and DLNs (af, pb1, pb2)

Cell no.	R_N (MΩ)	τ_m (ms)	Shunt factor	$r_{m,soma}$ (kΩ cm^2)	$r_{m,dend}$ (kΩ cm^2)	r_i (Ω cm)	c_m (μF/cm^2)
		2.4	10	352	3521	318	1.3
4/1	15.2	2.4	20	298	6258	370	1.0
		4.1	50	267	13599	371	1.9
		2.4	1	2407	2407	245	1.2
4/6	15.0	4.1	10	658	6579	422	1.9
		4.1	20	570	11981	406	1.4
		2.4	20	207	4340	311	1.3
7/4	14.6	2.4	30	194	6018	348	1.1
		2.4	40	188	7697	363	1.0
		3.0	1	1990	1990	208	1.6
af	1.9	3.0	20	358	7525	385	1.0
		4.5	50	305	15557	454	1.6
		3.0	1	1935	1935	191	1.7
pb1	1.7	3.0	30	202	6261	396	1.1
		4.5	50	181	9224	365	1.7
		3.0	1	1912	1912	207	1.7
pb2	3.6	3.0	10	382	3816	310	1.3
		4.5	60	232	14209	458	1.6

Delays. Delays are shorter in the mean for DLNs. The lowest delays were obtained with parameter combinations for the uniform case (shunt factor = 1). If $R_{\mathrm{m},\,soma}$ is raised to the dendritic value $R_{\mathrm{m},\,dend}$ for cases with shunt factors > 1, mean local delay increases distinctly, since local delay at soma and stem dendrites is incremented. The higher the shunt factor, the higher were the local delays (LDs). The largest LDs were determined in SLNs with very small dendritic diameters (diameter of terminals < 1 μm) and high values of $R_{\mathrm{m},\,dend}$. The mean calculated transfer delay (TD) in SLNs is up to 5 times higher than in DLNs (Table 3).

Time window. On the average, time windows ($2\widehat{\sigma}_f$) at soma are somewhat greater in SLNs while they agree on dendrites for both groups. More distinct differences are uncovered if time windows and signal delays are compared. For SLNs, the ratio of time window at soma to transfer delay is about 1 : 2, but for DLNs it is 1 : 1 (Tables 3 and 4).

This means, in relation to their transfer delays to soma, SLNs have short time windows at soma. Hence, incoming signals went already down at soma when soon thereafter other signals arrive. For DLNs, transfer delays to soma and time windows at soma are of the same order of magnitude in the mean. That is, at any time a substantial number of incoming signals may be expected to sum up at soma.

5. Conclusion

We studied the question to what extent DLNs and SLNs can be treated as integrators summing up a number of small synaptic inputs over some characteristic period, or as coincidence detectors which fire when a few synaptic inputs arrive at the trigger zone within that period. Our simulations showed that a complex relationship between dendritic branching pattern and neuron function exists.

Attenuation of signals is generally larger in SLNs. Nonlinear amplification mechanisms in the dendrites must be operating, or localized integration of postsynaptic signals in clusters must take place, if the soma or initial segment of the neuron should

Table 3
Transfer delay (mean and SD) to soma in SLNs (left) and DLNs (right)

Cell ID	Mean (ms)	SD (ms)	Cell ID	Mean (ms)	SD (ms)
41–318	10.9	5.7	af–208	3.8	0.8
41–370	10.4	5.5	af–385	4.0	1.2
41–371	34.5	18.6	af–454	7.6	2.6
46–245	7.5	3.2	pb1–191	4.0	1.0
46–422	22.9	11.0	pb1–396	4.4	1.4
46–406	22.5	10.9	pb1–365	8.0	2.6
74–311	7.5	5.2	pb2–207	3.7	0.9
74–348	7.3	5.3	pb2–310	3.8	1.2
74–363	7.1	5.1	pb2–458	7.2	2.8

Table 4
Time window is SLNs and DLNs. Displayed are means of $2\widehat{\sigma}_f$ and standard deviation SD at soma and at dendritic sites

Cell ID	Time window at soma (ms)			Dendritic time window (ms)		
	Mean	SD	Max	Mean	SD	Max
41–318	5.6	1.4	9.6	3.5	0.5	4.4
41–370	5.9	1.5	10.4	3.8	0.6	4.9
41–371	20.5	5.7	34.3	12.9	2.8	19.4
46–245	4.2	0.8	6.3	2.6	0.3	3.5
46–422	12.5	3.2	21.2	7.4	1.3	9.5
46–406	14.0	3.5	23.9	8.9	1.8	12.2
74–311	4.9	1.7	9.3	3.5	0.8	4.9
74–348	5.1	1.8	9.9	3.7	1.0	5.3
74–363	5.1	1.8	9.8	3.8	1.0	5.5
af–208	3.6	0.2	4.3	2.1	0.3	3.3
af–385	3.9	0.4	5.6	2.4	0.4	3.8
af–454	7.1	1.0	11.6	4.0	1.2	8.5
pb1–191	3.7	0.2	4.9	2.1	0.3	3.5
pb1–396	4.1	0.5	5.6	2.6	0.5	4.4
pb1–365	7.3	1.0	10.5	4.1	1.1	8.1
pb2–207	3.6	0.2	4.1	2.3	0.4	3.3
pb2–310	3.7	0.4	4.6	2.4	0.4	3.3
pb2–458	7.2	1.1	10.1	4.3	1.3	7.7

be affected. The findings on time windows and transfer delays suggest that only temporally at soma coinciding signals will influence it.

For DLNs, attenuation of signals is much less. The relation of time windows and transfer delays is such that incoming signals can be summed up over a period of the order of time constant. Hence, an integrator function in DLNs seems plausible.

These findings hold for the various sets of admissible parameter combinations used in this study. While the order of magnitude of the results depends on the set of parameters used in the forward computations, their relation within a cell group is barely affected. The differences revealed between the two groups, however, are even amplified in some cases.

References

[1] H. Agmon-Snir, A novel theoretical approach to the analysis of dendritic transients, Biophys. J. 69 (1995) 1633–1656.

[2] R. Grantyn, A. Grantyn, A. Schierwagen, Passive membrane properties, afterpotentials and repetitive firing of superior colliculus neurons studied in the anesthetized cat, Brain Res. 50 (1983) 377–391.

[3] R. Grantyn, R. Ludwig, W. Eberhardt, Neurons of the superficial tectal gray. An intracellular HRP-study on the kitten superior colliculus in vitro, Exp. Brain Res. 55 (1984) 172–176.
[4] M. Ohme, A. Schierwagen, A method for analysing transients in dendritic trees with nonuniform segments, in: R. Trappl (Ed.), Cybernetics and Systems '96, Austrian Society for Cybernetic Studies, Vienna, 1996, pp. 542–547.
[5] A. Schierwagen, Distributed parameter systems as models of current flow in nerve cells with branched dendritic trees: inverse and forward problems, Syst. Anal. Model. Simul. 5 (1988) 453–471.
[6] A. Schierwagen, R. Grantyn, Quantitative morphological analysis of deep superior colliculus neurons stained intracellularly with HRP in the cat, J. Hirnforsch. 27 (1986) 611–623.
[7] A. Schierwagen, Segmental cable modelling of electrotonic transfer properties of deep superior colliculus neurons in the cat, J. Hirnforsch. 27 (1986) 679–690.
[8] J. van Pelt, A. Schierwagen, H.B.M. Uylings, Modeling dendritic morphological complexity of cat superior colliculus neurons, Neurocomputing 38–40 (2001) 403–408, this issue.

Andreas Schierwagen was born in Dresden, Germany, in 1945. He received his doctorate in Mathematics from the Friedrich Schiller University Jena in 1974. He is currently Professor of the Institute of Computer Science at the University of Leipzig. His current research areas include information processing in single neurons and in neural fields.